Effects of Cu on the martensitic transformation and magnetic properties of $Mn_{50}Ni_{40}In_{10}$ alloy*

Li Ge-Tian(李歌天)[a], Liu Zhu-Hong(柳祝红)[a]†, Meng Fan-Yan(孟凡研)[a], Ma Xing-Qiao(马星桥)[a], and Wu Guang-Heng(吴光恒)[b]

[a] *Department of Physics, University of Science and Technology Beijing, Beijing* 100083, *China*

[b] *Beijing National Laboratory for Condensed Matter Physics, Institute of Physics, Chinese Academy of Science, Beijing* 100190, *China*

(Received 11 August 2013; revised manuscript received 29 September 2013)

The structures, the martensitic transformations, and the magnetic properties are studied systematically in $Mn_{50}Ni_{40-x}Cu_xIn_{10}$, $Mn_{50-x}Cu_xNi_{40}In_{10}$, and $Mn_{50}Ni_{40}In_{10-x}Cu_x$ alloys. The partial substitution of Ni by Cu reduces the martensitic transformation temperature, but has little influence on the Curie temperature of austenite. Comparatively, the martensitic transformation temperature increases and the Curie temperature of austenite decreases with the partial replacement of Mn or In by Cu. The magnetization difference between the austenite phase and the martensite phase reaches 70 emu/g in $Mn_{50}Ni_{39}Cu_1In_{10}$; a field-induced martensite-to-austenite transition is observed in this alloy.

Keywords: shape-memory effect, martensitic transformations, intermetallic compounds

PACS: 62.20.fg, 81.30.Kf, 71.20.Lp **DOI:** 10.1088/1674-1056/22/12/126201

1. Introduction

Heusler alloys $Ni_{50}Mn_{50-x}Z_x$ (Z = In, Sn, Sb)[1–8] have received much attention due to high performances of actuator and sensor materials since a magnetic-field-induced martensite-to-austenite transformation was realized in these alloys. These alloys present a structural transition from a ferromagnetic parent phase to an antiferromagnetic-like or ferromagnetic martensite phase,[9,10] exhibiting a large saturation magnetization difference (ΔM) between the martensite and austenite phase. Thus, a magnetic field-induced reverse martensitic transformation can be achieved. In the NiMn-based Heusler alloy Ni_2MnZ, the magnetic moment is mainly confined to Mn atoms and the magnetism is thought to arise from the Ruderman–Kittel–Kasuya–Yosida (RKKY) exchange interaction mediated by the conduction electrons.[11] Recently, Mn-rich alloys Mn_2NiX (X = Ga, In, Sn)[12–15] have been developed; these alloys have obvious advantages with the increase of the Mn content in the matrix. However, only a small ΔM of ∼9 emu/g was obtained in the Mn_2NiGa alloy,[16] which can be enhanced to 30 emu/g by partially doping Ni with Co in $Mn_{48}Co_xNi_{32-x}Ga_{20}$ alloys.[17] In $Mn_{50}Ni_{40}In_{10}$[9,18] ribbon alloy, a ΔM of 40 emu/g was achieved. A complete reversible metamagnetic transformation was realized in the $Mn_{50}Ni_{37}In_{10}Co_3$ polycrystalline alloy.[19] A significant net increase of 40 emu/g is gained for ΔM of $Mn_{50}Ni_{40}In_{10}$. It has been found that the Cu addition is effective to enhance the magnetocaloric effect in the Ni_2MnGa alloy[20] due to the improvement in magnetization. A magnetic-field-driven martensitic transformation was also implemented in a Cu-doped $Ni_{50}Mn_{33}Ga_{17}$ alloy.[21] Very recently, it was suggested that the hybridization between Ni 3d states and Mn 3d states played an important role in the martensitic transformation of Mn-rich alloys.[22] It seems that the introduction of Cu enhances the extent of the covalent hybridization between Ni(d states)-Ga(p states) in $Ni_2Mn_{1-x}Cu_xGa$ alloys.[23] Simultaneously, the magnetic moment of the NiMn-based Heusler alloy is mediated by the p–d hybridization. Therefore, it is necessary to study the influences of Cu on the martensitic transformation and magnetic properties in NiMn-based Heusler alloys. In this paper, we study the martensitic transformation and magnetic properties of the Cu-doped $Mn_{50}Ni_{40}In_{10}$ alloy. The physical mechanisms of Cu tailoring the transformation and magnetism are discussed in three systems of $Mn_{50}Ni_{40-x}Cu_xIn_{10}$ $Mn_{50-X}Cu_xNi_{40}In_{10}$, and $Mn_{50}Ni_{40}In_{10-x}Cu_x$.

2. Experiments

Three series of samples with nominal composition of $Mn_{50}Ni_{40-x}Cu_xIn_{10}$ (x = 0, 0.3, 1, 2), $Mn_{50}Ni_{40}In_{10-x}Cu_x$ (x = 0, 0.2, 0.4, 1, 2), and $Mn_{50-x}Cu_xNi_{40}In_{10}$ (x = 0, 1, 3, 4) were prepared using an arc melting furnace in an argon atmosphere from high purity (99.99%) elemental metals. The button shaped ingot (∼5.5 g) was melted four times in the furnace and heat treated at 1073 K for 24 hours in a vacuum, then slowly cooled down to room temperature to ensure the composition homogeneity. The compositions of all samples were determined by X-ray energy dispersive spectrometry (EDS);

*Project supported by the National Natural Science Foundation of China (Grant Nos. 51001010 and 11174030), the Research Fund for the Doctoral Program of Higher Education of China (Grant No. 20100006120001), and the Scientific Research Foundation for the Returned Overseas Chinese Scholars, State Education Ministry of China.

†Corresponding author. E-mail: zhliu_info@yahoo.com

© 2013 Chinese Physical Society and IOP Publishing Ltd

the results are collected in Table 1. The values of corresponding valence electron concentration e/a (electrons per atom) are also given in the table. The e/a was calculated on the assumption that the configurations of the valence electrons for Mn, Ni, In, Cu are $3d^5 4s^2$, $3d^8 4s^2$, $5s^2 5p^1$ and $3d^{10} 4s^1$ respectively. The crystal structures of the samples were determined by X-ray diffraction (XRD) using Cu-Kα radiation. The transformation behavior was studied through an alternating current (ac) susceptibility measurement with an ac field of 796 A/m and a frequency of 77 Hz. The magnetic properties were studied using a vibrating sample magnetometer (VSM) under a magnetic field of 3 T. The heating and cooling rates for M–T curves were both 1 K/min.

Table 1. Compositions of the samples determined by EDS analyses and the valence electron concentrations per atom e/a determined as the concentration-weighted sum of the s, d, and p electrons.

Nominal composition	Mn	Ni	In	Cu	e/a
$Mn_{50}Ni_{40-x}Cu_xIn_{10}$					
$x = 0$	49.7	40.3	10	0	7.809
$x = 0.3$	49.4	40.5	9.7	0.4	7.843
$x = 1$	49.3	40	9.7	1	7.852
$x = 2$	49.8	38.5	9.7	2	7.847
$Mn_{50-x}Cu_xNi_{40}In_{10}$					
$x = 0$	49.7	40.3	10	0	7.809
$x = 1$	48.9	40.8	9.5	0.8	7.876
$x = 3$	46.1	41	9.8	3.1	7.962
$x = 4$	44.4	41.4	10.1	4.1	8.002
$Mn_{50}Ni_{40}In_{10-x}Cu_x$					
$x = 0$	49.7	40.3	10	0	7.809
$x = 0.2$	49.7	40.5	9.6	0.2	7.839
$x = 0.4$	49.4	40.6	9.6	0.4	7.850
$x = 1$	48.5	41.9	8.6	1	7.953

3. Results and discussion

3.1. Structure

Figure 1(a) shows the XRD patterns for ingot samples of $Mn_{50}Ni_{40-x}Cu_xIn_{10}$ ($x = 0$, 0.3, 1, 2). All the Cu addition samples show the same XRD characteristic peaks as those of the parent sample $Mn_{50}Ni_{40}In_{10}$. They show a single bcc phase structure with fundamental lattice reflections of plane (220), (400), (422). For the $Mn_{50}Ni_{40}In_{10}$ sample, the crystal structure has been determined to be cubic with the parameter $a = 0.6009$ nm, which accords with the result of 0.6013 nm reported by Sanchez Llamazares *et al.*[9] in the $Mn_{50}Ni_{40}In_{10}$ ribbon sample. The partial substitution of Ni by Cu causes the lattice to shrink because the ion diameter of Cu is smaller than that of Ni. For example, the lattice parameter of $Mn_{50}Ni_{39.7}Cu_{0.3}In_{10}$ is $a = 0.6006$ nm, which is smaller than the 0.6009 nm of the $Mn_{50}Ni_{40}In_{10}$ alloy. As the Cu content increases to $x = 2$, there is an abnormal increase in the lattice parameter. When Cu partially replaces Mn, for $Mn_{50-x}Cu_xNi_{40}In_{10}$ ($x = 0$, 1, 3, 4) system, all these samples show the pure cubic austenite structures as shown in Fig. 1(b). The lattice parameters for all the samples are summarized in Table 2. It can be seen that the lattice parameters decrease with the increase of the Cu content, which results from the smaller atomic radius of Cu than that of Mn. For $Mn_{50}Ni_{40}In_{10-x}Cu_x$ ($x = 0$, 0.2, 0.4, 1, 2) systems, the lattice constants of the austenitic phase become smaller when replacing In with Cu due to the smaller atomic radius of Cu, as shown in Fig. 1(c) and Table 2. The unit cell parameter for $x = 0.2$ is $a = 0.5996$ nm. When the Cu content increases to $x = 0.4$, the XRD spectrum presents a two-phase structure, showing a cubic austenite structure and a tetragonal martensite structure. The lattice parameters for martensite are $a = 0.5528$ nm and $c = 0.6937$ nm. When the Cu content further increases to $x = 1$, the XRD pattern is fully indexed to be the non-modulated tetragonal martensite, indicating a pure martensite phase at room temperature for the $Mn_{50}Ni_{40}In_9Cu_1$ sample. It is obvious that the partial substitution of In by Cu reduces the stabilization of the austenite.

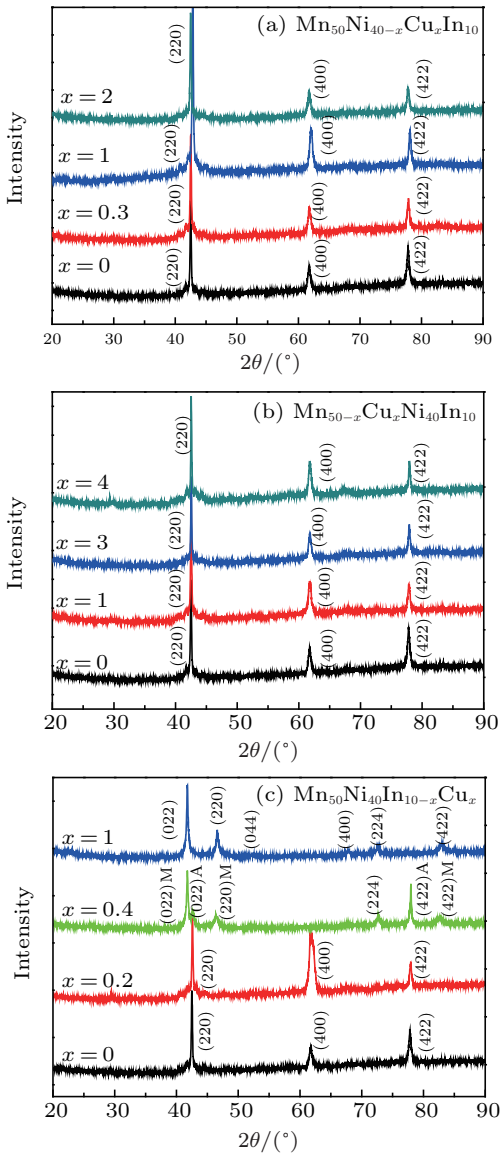


Fig. 1. (color online) X-ray diffraction patterns measured at room temperature for $Mn_{50}Ni_{40-x}Cu_xIn_{10}$ (a), $Mn_{50-x}Cu_xNi_{40}In_{10}$ (b) and $Mn_{50}Ni_{40}In_{10-x}Cu_x$ (c).

Table 2. Effects of Cu addition on the lattice parameters at room temperature.

Composition	Crystal phase	Lattice parameters		
		a/nm	*b*/nm	*c*/nm
$Mn_{50}Ni_{40-x}Cu_xIn_{10}$				
$x = 0$	Austenite	0.6009	0.6009	0.6009
$x = 0.3$	Austenite	0.6006	0.6006	0.6006
$x = 1$	Austenite	0.5977	0.5977	0.5977
$x = 2$	Austenite	0.6008	0.6008	0.6008
$Mn_{50-x}Cu_xNi_{40}In_{10}$				
$x = 0$	Austenite	0.6009	0.6009	0.6009
$x = 1$	Austenite	0.6005	0.6005	0.6005
$x = 3$	Austenite	0.6002	0.6002	0.6002
$x = 4$	Austenite	0.6001	0.6001	0.6001
$Mn_{50}Ni_{40}In_{10-x}Cu_x$				
$x = 0$	Austenite	0.6009	0.6009	0.6009
$x = 0.2$	Austenite	0.5996	0.5996	0.5996
	Austenite	0.5988	0.5988	0.5988
$x = 0.4$	Martensite	0.5528	0.5528	0.6937
$x = 1$	Martensite	0.5511	0.5511	0.6976

3.2. Martensitic transformation

Figure 2 shows the temperature dependences of ac susceptibility χ. Since the magnetic ordering follows the crystal lattice deformation, the martensitic transformation from the higher symmetry of cubic austenite to the lower symmetry of martensite is marked by a sharp drop of χ on cooling. It results from the enhancing of magnetocrystalline anisotropy at martensite. Therefore, the martensitic transformation temperature (T_M) and the Curie temperature of austenite (T_C) for samples have been accurately measured by this method. For $Mn_{50}Ni_{40-x}Cu_xIn_{10}$ ($x = 0$, 0.3, 1, 2) alloy systems, as shown in Fig. 2(a), the martensitic transformation occurs at 210 K for the $Mn_{50}Ni_{40}In_{10}$ sample. The martensitic transformation temperature T_M decreases rapidly to 160 K with the substitution of Ni by Cu at.1% and decreases to 100 K with further increase of the Cu content to at.2%. The martensitic transformation temperature T_M has an abnormal increase for the sample with $x = 0.3$ compared with for the sample $x = 0$. It is worth noting that T_C has little change with Cu addition; its value is $\sim$ 340 K as shown in Fig. 2(b).

For the $Mn_{50-x}Cu_xNi_{40}In_{10}$ ($x = 0$, 1, 3, 4) systems, as shown in Fig. 2(c), T_M increases with the partial substitution of Cu for Mn; the average increasing rate is $\sim$ 25 K per Cu addition. The Curie temperature of austenite T_C decreases with the partial substitution of Cu for Mn. T_M and T_C move towards each other with the increase of Cu content (see Fig. 2(d)). Except for the curve for the sample with $x = 0$, all the curves show a bending point during martensitic transformation, this may be attributed to two distinctive structural modulations changing with the martensitic transformation. It has also been observed in NiFeGa melt-spun ribbon;[24] a further TEM experiment is needed to clarify this point.

For $Mn_{50}Ni_{40}In_{10-x}Cu_x$ ($x = 0$, 0.2, 0.4, 1, 2) systems, as shown in Fig. 2(e), T_M increases while T_C decreases with the partial substitution of In by Cu. T_M and T_C merge at 322 K as the Cu increases to $x = 1$. Neither T_M nor T_C is detected in this curve when the Cu content further increases to $x = 2$. The XRD patterns confirm that the sample with $x = 2$ is in a martensite state, indicating that T_M increases up to a temperature higher than T_C. The variations of T_M and T_C with the increase of the Cu content are given in Fig. 2(f); it can be found that the change tendencies of T_M and T_C with the substitution of Cu for $Mn_{50-x}Cu_xNi_{40}In_{10}$ system accord with those in $Mn_{50}Ni_{40}In_{10-x}Cu_x$ samples. However, T_M and T_C have larger changes in $Mn_{50}Ni_{40}In_{10-x}Cu_x$ than in $Mn_{50-x}Cu_xNi_{40}In_{10}$ when the variation of x is equal.

The martensitic transformation temperature is generally attributed to the e/a ratio and unit cell volume change. Chernenko[25] found that T_M increases with the increase of e/a in Ni-Mn-Ga alloy. In $Ni_{50}Mn_{50-x}Z_x$ (Z = In, Sn, Sb) systems, Krenke *et al.*[26] also observed that T_M grows with the increasing of the e/a ratio. Jiang *et al.*[27] have proposed that the decreasing of unit cell volume[27] leads to the increase of T_M in a ferromagnetic shape memory alloy. From the view of the e/a, the replacement of an In ($5s^25p^1$) atom by a Cu ($3d^{10}4s^1$) atom results in an increase of eight valence electrons. From the perspective of the lattice volume, the substituting of a larger sized In atom with a smaller sized Cu atom results in the contraction of the unit cell, as has been observed in the XRD experiment. Both the increase of e/a and the decrease of the lattice volume make T_M increase in the $Mn_{50}Ni_{40}In_{10}$ alloy by the partial substitution of In by Cu. As Cu($3d^{10}4s^1$) substitutes for the Mn($3d^54s^2$) atom, the lattice parameter decreases from 0.6009 nm to 0.6001 nm in the Cu4 sample, and e/a increases simultaneously. Both factors make T_M increase. In the Cu-substituted Ni($3d^84s^2$) system, the e/a ratio is slightly increased and the unit cell volume is proved to slightly contract by the XRD results. If just the usual factors of the e/a ratio and the unit cell volume effect are considered, T_M should increase with the Cu content in the partially Cudoped Ni system. However, T_M is significantly reduced by partially replacing Ni with Cu in the $Mn_{50}Ni_{40}In_{10}$ alloy. A similar result has been reported in the $Ni_{50}Mn_{31}Ga_{19}$ alloy with partially Cudoped Ni; no analysis has been put forward about the abnormal result.[21] Theoretical calculation reveals that the main driving force for martensitic transformation in the Mn-rich Heusler alloy is the hybridization between Ni 3d e_g states and the 3d states of excess Mn at the Z position.[22] The substitution of Ni by Cu results in a decrease of Ni covalency and a weaker Ni–Mn (at the In position) chemical bond. A weaker degree of Ni–Mn (at the In position) hybridization just requires lower energy to induce the martensitic transformation, bringing about the decrease of T_M. The abnormal increase of T_M for a sample with $x = 0.3$ in the $Mn_{50}Ni_{40-x}Cu_xIn_{10}$ system may be due to the competition resulting between the unit cell effect on T_M and the hybridization effect on T_M.

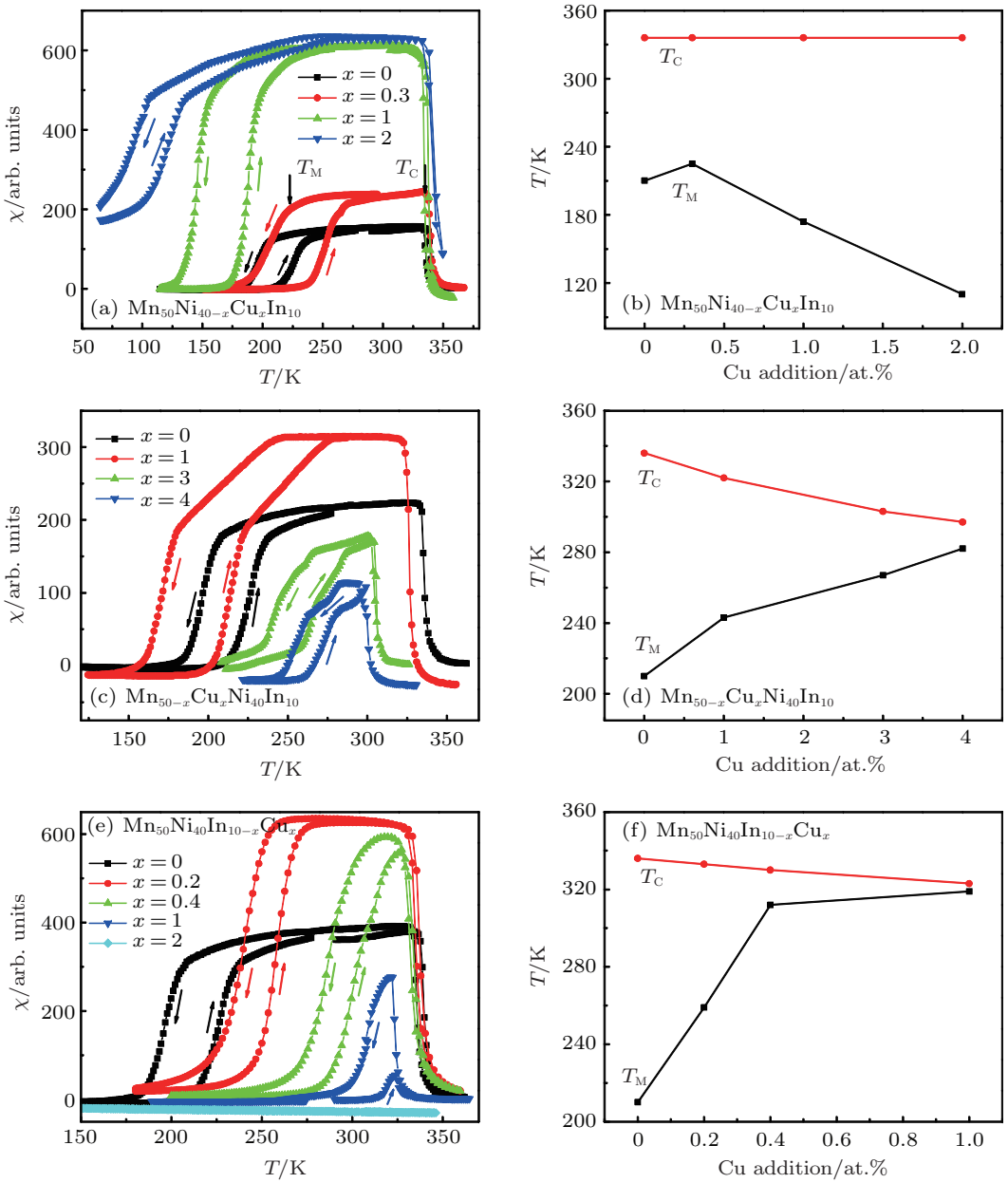


Fig. 2. (color online) Temperature dependences of ac susceptibility of $Mn_{50}Ni_{40-x}Cu_xIn_{10}$ (a), $Mn_{50-x}Cu_xNi_{40}In_{10}$ (c) and $Mn_{50}Ni_{40}In_{10-x}Cu_x$ (e) alloys and variations of the martensitic transformation temperature (T_M) and the Curie temperature of austenite (T_C) with the Cu content for $Mn_{50}Ni_{40-x}Cu_xIn_{10}$ (b), $Mn_{50-x}Cu_xNi_{40}In_{10}$ (d) and $Mn_{50}Ni_{40}In_{10-x}Cu_x$ (f) alloys.

3.3. Magnetic properties

Figure 3 shows the M–T curves measured under a magnetic field of 2 T. All the measurements were firstly conducted during heating after the samples had been cooled down from 390 K to 55 K under zero magnetic field and then conducted upon the cooling process from 390 K to 55 K. The abrupt changes in magnetization indicate the reverse martensitic transformations. The magnetization difference, ΔM, between the austenitic phase and the martensitic phase can be easily read from the curves. We use the heating curves to calculate ΔM in this paper. For the parent compound $Mn_{50}Ni_{40}In_{10}$, ΔM is 73 emu/g. By replacing Ni with Cu, as can be seen from Fig. 3(a), ΔM first decreases to 70 emu/g in the Cu1 sample and further decreases to 55 emu/g as the Cu content further increases to $x = 2$. For the samples with the partial substitution of Mn by Cu, ΔM decreases gradually from 66 emu/g to 38 emu/g as the Cu content increases from $x = 1$ to $x = 4$. In comparison, for $Mn_{50}Ni_{40}In_{10-x}Cu_x$ ($x = 0$, 0.2, 0.4, 1) systems, there is a great decrease in the magnetization of austenite with Cu content $x \geq 0.4$. However, all samples keep a low magnetization state at the martensite state, resulting in a rapid decrease of ΔM from 73 emu/g in $Mn_{50}Ni_{40}In_{10}$ to 11 emu/g in $Mn_{50}Ni_{40}In_9Cu_1$ (see Fig. 3(c)). Comparing the three studied systems, it can be found that the martensitic transformation temperature, Curie temperature, and magnetization are most sensitive to the Cu content in the $Mn_{50}Ni_{40}In_{10-x}Cu_x$ system. Only at.1% Cu doping can reduce T_M by about 110 K and ΔM by about 60 emu/g.

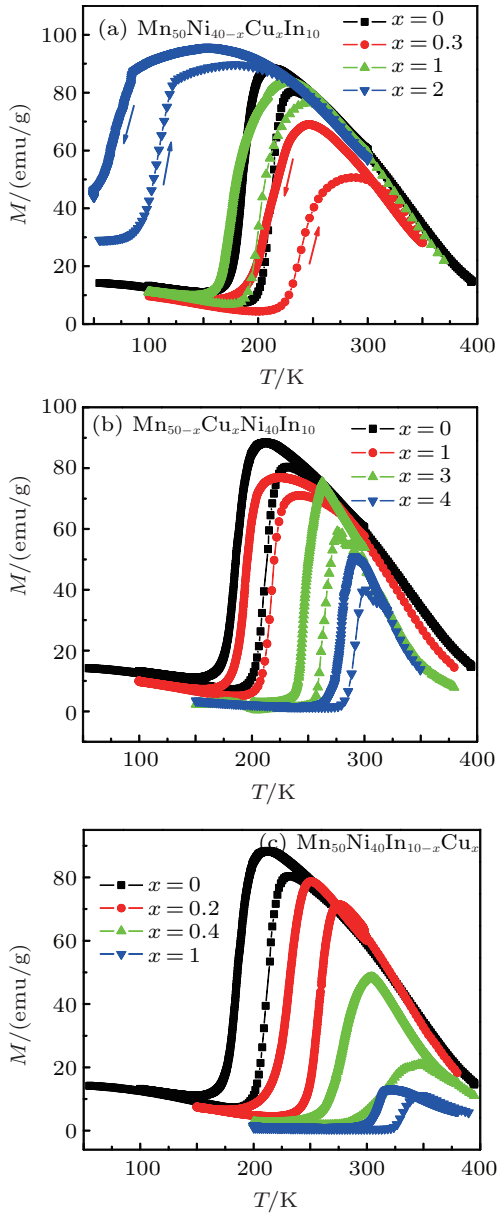


Fig. 3. (color online) M–T curves of $Mn_{50}Ni_{40-x}Cu_xIn_{10}$ (a), $Mn_{50-x}Cu_xNi_{40}In_{10}$ (b), and $Mn_{50}Ni_{40}In_{10-x}Cu_x$ (c) alloys measured under 20 kOe by VSM. The unit 1 Oe = 79.5775 A·m^{-1}.

Stearns[28] has investigated the magnetic behaviors in Heusler alloys in detail; he proposed that the transition metals Mn, Fe, Co, and Ni each have a small portion of itinerant 3d electrons (d_i) per atom besides the localized 3d electrons (d_l) and the larger the atomic number, the fewer d_i electrons they have in the same period. The magnetic behavior of the Heusler alloy is controlled by three types of magnetic interaction: (i) an s–d_l interaction between s-like conduction electrons and localized d_l electrons via Coulomb exchange and hybridization, (ii) a d_i–d_l interaction between iterant d electrons (d_i) and localized d electrons (d_l), and (iii) a superexchange interaction through the sp elements at the Z sites. This interaction takes place through the p electrons and is usually antiferromagnetic. In ferromagnetic Heusler alloys, the d_i–d_l interaction is thought to be dominant, while in antiferromagnetic alloys, s conduction electron polarization and superexchange interaction are thought to be dominant. Owing to the partial sustitution of Ni by Cu, the number of d_i decreases and the number of d_l increases, thus the d_i–d_l interaction and s–d_l interaction are affected. Because of the partial replecement of Mn by Cu, the number of d_i decreases and the number of d_l increases, more than in the Cu-doped Ni case. As Cu partially substitutes for In, the In p states change, resulting in the change of the superexchange interaction. The overall magnetization originates from the competition among the d_i–d_l interaction, the s–d_l, and superexchange interaction. From Figs. 3(b) and 2(b), it seems that the overall magnetization and T_C decrease with Mn partially replaced by Cu in $Mn_{50}Ni_{40}In_{10}$, indicating that the d_i–d_l interaction is reduced by the Cu addition. For the Cu-doped partial In system, it is the change of the superexchange interaction that reduces the Curie temperature and the magnetization. In fact, the magnetic interaction is complex in these systems and it is difficult to exactly clarify the details for magnetic interaction at this moment. Deep electronic structure calculations are required to elucidate the electron exchange mechanism in these alloys.

The Cu-substitued partial Ni system has a large ΔM compared with other two alloy-systems, so we measured the isothermal magnetization curves for the $Mn_{50}Ni_{39}CuIn_{10}$ alloy as shown in Fig. 4. When the temperature is lower than the value for the reverse martensitic transformation, i.e. 165 K, the sample shows a typical soft magnetic behavior with a saturation magnetization of 15 emu/g under the action of 3 T. From 194 K to 206 K, the jump-like magnetization change was obtained during the magnetizing and a large hysteresis between magnetizing and demagnetizing process was observed, owing to the occurrence of the metamagnetic transformation. Particularly for 202 K, the reverse martensitic phase transformation was induced at 0.8 T, indicating the potential application for magnetic actuation.

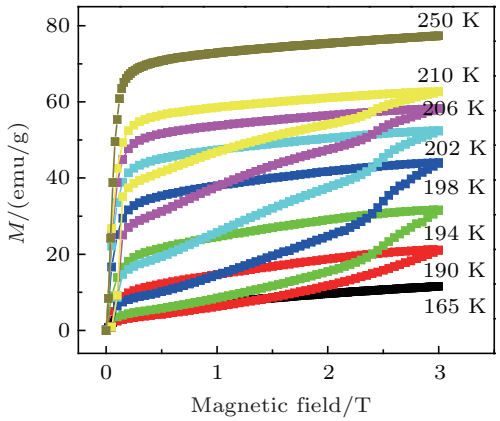


Fig. 4. (color online) Isothermal magnetization loops of the $Mn_{50}Ni_{39}CuIn_{10}$ alloy at different temperatures.

4. Conclusions

In the present paper, we have investigated the structures and the magnetic and martensitic transformation prop-

erties of the $Mn_{50}Ni_{40-x}Cu_xIn_{10}$, $Mn_{50-x}Cu_xNi_{40}In_{10}$, and $Mn_{50}Ni_{40}In_{10-x}Cu_x$ alloys. Based on the obtained experimental results, some conclusions may be drawn.

i) The martensitic transformation temperature T_M increases and the Curie temperature for austenite T_C decreases with the partial substitution of Mn or In by Cu in $Mn_{50}Ni_{40}In_{10}$, while T_M decreases rapidly with the increase of the Cu content partially replacing Ni. The decrease of T_M in the Cu-substituted Ni system is attributed to the weakening of the hybridization between Ni and Mn (at the In site).

ii) The magnetization change in Cu-alloyed $Mn_{50}Ni_{40}In_{10}$ is mainly attributed to the competition result among s–d_l, d_l–d_i and the superexchange interaction.

iii) A field-induced martensite-to-austenite transition is observed in the $Mn_{50}Ni_{39}Cu_1In_{10}$ alloy due to a large magnetization difference of 70 emu/g between the austenite phase and the martensite phase, implying that quaternary alloys are the new candidate materials for actuators.

References

[1] Kainuma R, Imano Y, Ito W, Sutou Y, Morito H, Okamoto S, Kita-kami O, Oikawa K, Fujita A, Kanomata T and Ishida K 2006 *Nature* **439** 957

[2] Yu S Y, Liu Z H, Liu G D, Chen J L, Cao Z X, Wu G H, Zhang B and Zhang X X 2006 *Appl. Phys. Lett.* **89** 162503

[3] Ito W, Xu X, Umetsu R Y, Kanomata T, Ishida K and Kainuma R 2011 *J. Appl. Phys.* **109** 07A926

[4] Koyama K, Okada H, Watanabe K, Kanomata T, Kainuma R, Ito W, Oikawa K and Ishida K 2006 *Appl. Phys. Lett.* **89** 182510

[5] Umetsu R Y, Sheikh A, Ito W, Ouladdiaf B, Ziebeck K R A, Kanomata T and Kainuma R 2011 *Appl. Phys. Lett.* **98** 042507

[6] Li P P, Wang J M and Jiang C B 2011 *Chin. Phys. B* **20** 028104

[7] Hu F X, Shen B G and Sun J R 2013 *Chin. Phys. B* **22** 037505

[8] Tian X H, Sui J H, Zhang X, Feng X and Cai W 2011 *Chin. Phys. B* **20** 047503

[9] Sánchez Llamazares J L, Sanchez T, Santos J D, Pérez M J, Sanchez M L, Hernando B, Escoda Ll, Suño J J and Varga R 2008 *Appl. Phys. Lett.* **92** 012513

[10] Krenke T, Acet M, Wassermann E, Moya X, Mañosa L and Planes A 2006 *Phys. Rev. B* **73** 174413

[11] Johnston G B and Hall E O 1968 *J. Phys. Chem. Solids* **29** 193

[12] Barman S R, Ranik S, Shukla A K, Kamal C and Charkrabarti A 2007 *Europhys. Lett.* **80** 57002

[13] Sanjay Singh, Maniraj M, D'Souza S W, Ranjan R and Barman S R 2010 *Appl. Phys. Lett.* **96** 081904

[14] Liu G D, Dai X F, Liu H Y, Chen J L, Li Y X, Xiao G and Wu G H 2008 *Phys. Rev. B* **77** 014424

[15] Wu Z G, Liu Z H, Yang H, Liu Y and Wu G H 2011 *Intermetallics* **19** 1839

[16] Liu G D, Chen J L, Liu Z H, Dai X F and Wu G H 2005 *Appl. Phys. Lett.* **87** 262504

[17] Ma L, Zhang H W, Yu S Y, Zhu Z Y, Chen J L, Wu G H, Liu H Y, Qu J P and Li Y X 2008 *Appl. Phys. Lett.* **92** 032509

[18] Sánchez Llamazares J L, Hernando B, Prida V M, Garcia C, Gonzalez J, Varga R and Ross C A 2009 *J. Appl. Phys.* **105** 07A945

[19] Wu Z G, Liu Z H, Yang H, Liu Y and Wu G H 2011 *Appl. Phys. Lett.* **98** 061904

[20] Stadler S, Khan M, Mitchell J, Ali N, Gomes A M, Dubenko I, Takeuchi A Y and Guimarães A P 2006 *Appl. Phys. Lett.* **88** 192511

[21] Jiang C B, Wang J M, Li P P, Jia A and Xu H B 2009 *Appl. Phys. Lett.* **95** 012501

[22] Mahmud Khan, Jung J, Stoyko S S, Arthur Mar, Abdiel Quetz, Tapas Samanta, Igor Dubenko, Naushad Ali, Shane Stadler and Chow K H 2012 *Appl. Phys. Lett.* **100** 172403

[23] Sharma V K, Chattopadhyay M K, Khandelwal A and Roy S B 2010 *Phys. Rev. B* **82** 172411

[24] Li J Q, Liu Z H, Yu H C, Zhang M, Zhou Y Q and Wu G H 2003 *Solid State Commun.* **126** 323

[25] Chernenko V A 1999 *Scr. Mater.* **40** 523

[26] Krenke T, Moya X, Aksoy S, Acet M, Entel P, Mañosa L I, Planes A, Elerman Y, Yücel A and Wassermann E F 2007 *J. Magn. Magn. Mater.* **310** 2788

[27] Jiang C B, Feng G, Gong S K and Xu H B 2003 *Mater. Sci. Eng. A* **342** 231

[28] Sterns M B 1979 *J. Appl. Phys.* **50** 2060